Estimation of Bearing Capacity of Circular Footings on Sands Based on Cone Penetration Test

Junhwan Lee[1] and Rodrigo Salgado[2]

Abstract: In the present paper, the estimation of limit unit bearing capacity q_{bL} of axially loaded circular footings on sands based on cone penetration test cone resistance q_c is examined. There are significant uncertainties in the calculation of bearing capacity using the bearing capacity equation. The selection of the value of the soil friction angle ϕ and of the equation for N_γ accounts for much of the overall uncertainty. The approach proposed in this study can reduce the uncertainties associated with the bearing capacity equation, as no estimation of ϕ or selection of an equation for N_γ is necessary. Instead, normalized limit unit bearing capacities q_{bL}/q_c are calculated from non-linear finite element and cone penetration resistance analyses for various soil and footing conditions. Effects of the relative density D_R, the lateral earth pressure ratio K_0, and the footing size are also addressed. It is observed that the normalized limit unit bearing capacity q_{bL}/q_c decreases as D_R increases and that this rate of decrease of q_{bL}/q_c varies with K_0. Values of q_{bL}/q_c are presented both in equation form and in charts. The values of normalized allowable unit load $q_{b,\text{all}}/q_c$ at a settlement of 25 mm for various soil and stress states are also provided.

DOI: 10.1061/(ASCE)1090-0241(2005)131:4(442)

CE Database subject headings: Footings; Bearing capacity; Foundation design; Sand; Settlement.

Introduction

The bearing capacity problem of footings has been extensively studied for many decades. The bearing capacity equation expresses the unit load that would cause a footing to plunge into the ground as a function of the cohesive intercept c, the surcharge q at the level of the footing base, and the unit weight γ. A variety of factors, all functions of ϕ, appear in each term; in particular, factors N_c, N_q, and N_γ appear multiplying c, q, and γ, respectively. The pioneering work by Prandtl (1921) and Reissner (1924) established the values of the bearing capacity factors N_c and N_q, and most efforts since have focused on the evaluation of the bearing capacity factor N_γ and correction factors associated with footing embedment, footing shape, and other complications (Terzaghi 1943; Brinch Hansen 1970; Vesic 1973; Kumbhojkar 1993; Michalowski 1997; Zhu et al. 2001).

For the limit unit bearing capacity q_{bL} of footings, important issues to be addressed include conservatism and uncertainty. The bearing capacity equation is based on the assumption of superposition of the c, q, and γ terms. This assumption leads to conservative values of q_{bL} (Griffiths 1982; Bolton and Lau 1993). The uncertainty results in large part from the uncertainties in the estimation of ϕ and in the expression for N_γ. While the expressions for N_c and N_q are exact, there is no exact equation for N_γ. Additional uncertainty results from the expressions for the shape, depth, load inclination, and base and ground inclination factors, which are also approximate.

In addition to the uncertainty when estimating ϕ from a given input, say relative density D_R, the mobilized friction angle along the slip surface is not the same due to different dilatancy rates. This increases the uncertainty in the value of ϕ to use in the bearing capacity equation, although the literature contains procedures for selection of values of the friction angle ϕ that attempt to account for such effects (e.g., Perkins and Madson 2000).

According to Griffith (1982), the factor N_γ represents the effect of the effective stress field below the footing base on q_{bL}, and the initial value of the coefficient of lateral earth pressure K_0, as a result, should affect the bearing capacity. However, using the two theorems of limit analysis (Drucker et al. 1952) to guide us, a different conclusion may be reached. From an upper bound point of view, the body forces are strictly vertical (gravity) forces; thus, in a cohesionless soil, gravity is the only source of resistance to collapse, and the values of the lateral stresses should not matter. From a lower bound point of view, the stress field that matters is one that is very close to collapse. So, again, K_0 does not matter. So it seems that the only influence of K_0 would be through the value of the resulting ϕ value, which would be slightly less for a higher K_0 value due to the increased confinement. Values of K_0 for most sandy soils lie within the 0.4–0.5 range. The value of $K_0=1.0$ may be regarded as the upper limit for highly overconsolidated sands. An investigation of the effects of K_0 on the bearing capacity is also desirable for improved designs.

The other uncertainty associated with N_γ is in the evaluation of size effects. It has been shown and is intuitive that N_γ varies with footing size, as the friction angle ϕ decreases with the increasing confining stress associated with larger footings (Zhu et al. 2001).

In the present study, the evaluation of footing bearing capacity is examined with the aim to reduce these uncertainties. A method

[1]Associate Professor, School of Civil & Environmental Engineering, Yonsei Univ., Seoul, South Korea. E-mail: junlee@yonsei.ac.kr

[2]Professor, School of Civil Engineering, Purdue Univ., West Lafayette, IN 47907-1284. E-mail: rodrigo@ecn.purdue.edu

Note. Discussion open until September 1, 2005. Separate discussions must be submitted for individual papers. To extend the closing date by one month, a written request must be filed with the ASCE Managing Editor. The manuscript for this paper was submitted for review and possible publication on March 17, 2003; approved on August 9, 2004. This paper is part of the ***Journal of Geotechnical and Geoenvironmental Engineering***, Vol. 131, No. 4, April 1, 2005. ©ASCE, ISSN 1090-0241/2005/4-442–452/$25.00.

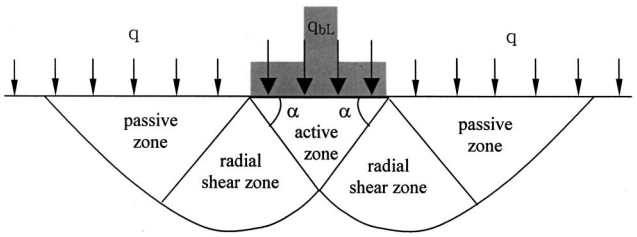

Fig. 1. Typical failure mechanism of axially loaded footing

for estimating q_{bL} directly from cone penetration test (CPT) cone resistance q_c is proposed. The analysis focuses on axially loaded circular footings bearing on sand. The loading response of the footings in sand is simulated using the finite element method. Various soil conditions, with different D_R and K_0 values, are considered.

Bearing Capacity Solutions for Footings

The bearing capacity equation for footings bearing on sand is

$$q_{bL} = qN_q s_q d_q i_q g_q b_q + \tfrac{1}{2}\gamma B N_\gamma s_\gamma d_\gamma i_\gamma g_\gamma b_\gamma \tag{1}$$

where q_{bL}=limit unit bearing capacity; q=surcharge at footing base level; γ=unit weight of foundation soil; B=footing size; N_q and N_γ=bearing capacity factors; and s, d, i, g, and b=shape, depth, load inclination, ground inclination, and base inclination factors, respectively. A wide range of N_γ values exists from solutions based on limit equilibrium, limit analysis, and other numerical methods. The expression for N_q, which is exact for weightless soil, is

$$N_q = \frac{1+\sin\phi}{1-\sin\phi} e^{\pi \tan\phi} \tag{2}$$

The limit equilibrium method has been the most commonly used method to evaluate the bearing capacity of footings due to its simplicity (Terzaghi 1943; Vesic 1973; Kumbhojkar 1993; Zhu et al. 2001). According to typical slip patterns for limit equilibrium approaches shown in Fig. 1, a failure zone can be divided into active, radial shear, and passive zones. Zhu et al. (2001) performed limit equilibrium analyses using slip patterns with the angle α of the active zone equal to ϕ, $45°+\phi/2$, and an angle giving the minimum N_γ value. The resulting equations for N_γ, corresponding to $\alpha=\phi$, $45°+\phi/2$, and the angle minimizing N_γ, are given by

$$N_\gamma = (2N_q+1)(\tan\phi)^{1.35} \tag{3}$$

$$N_\gamma = (2N_q+1)(\tan 1.07\phi) \tag{4}$$

$$N_\gamma = (2N_q+1)(\tan\phi)^{1.45} \tag{5}$$

The limit equilibrium approach does not produce mechanically rigorous solutions. Limit analysis solutions, on the other hand, are rigorous in the sense that the stress field of a lower bound solution is in equilibrium with imposed loads at the boundaries of the soil mass, while the velocity field of an upper bound solution is compatible with imposed velocities. The upper bound approach has frequently been used in the solution of footing bearing capacity problems (Chen 1975; Sloan and Yu 1996; Michalowski 1997; Soubra 1999; Zhu 2000). Michalowski (1997) presented equations for N_γ developed for rough and smooth footings, respectively, based on upper bound solutions assuming multiblock failure mechanisms

$$N_\gamma = e^{0.66+5.11\tan\phi}\tan\phi \tag{6}$$

$$N_\gamma = e^{5.1\tan\phi}\tan\phi \tag{7}$$

The finite element and finite difference methods have been the most common numerical methods for analysis of the loading response and bearing capacity of footings (Griffths 1982; Frydman and Burd 1997; Erickson and Drescher 2002). Griffiths (1982) used the finite element analysis for the determination of the bearing capacity factors and assessment of the Terzaghi bearing capacity equation. Values of the bearing capacity factors evaluated by Griffiths (1982) are in good agreement with those obtained by Prandtl (1921) and Terzaghi (1943) using limit equilibrium methods. Frydman and Burd (1997) and Erickson and Drescher (2002) performed finite difference analyses. Results of the analyses showed that the bearing capacity factors increase as the soil dilatancy angle ψ increases. This also indicates that the dilatancy angle ψ should be considered in the estimation of bearing capacity when high accuracy is needed.

Numerical Simulation of Footing Load Tests

A modern design concept in geotechnical engineering is to treat serviceability and ultimate limit states within the same framework. In this integrated framework, the stability and functionality of foundations are not independent, and both strength and stiffness are properly taken into account. In this study, therefore, the numerical simulation of footing load response and bearing capacity is based on a stress–strain model that represents the pre- and postfailure behavior of soils realistically, considering the nonlinearity of soil stiffness and strength.

Nonlinear Stiffness and Strength Model

Based on the observed degradation of elastic modulus in sands, Lee and Salgado (2000) suggested the following modulus degradation relationship for a general stress state:

$$\frac{G}{G_0} = \left[1 - f\left(\frac{\sqrt{J_2}-\sqrt{J_{20}}}{\sqrt{J_{2\,\max}}-\sqrt{J_{20}}}\right)^g\right]\left(\frac{I_1}{I_{10}}\right)^{n_g} \tag{8}$$

where G_0 and G=initial and secant shear modulus; J_2 J_{20}, and $J_{2\max}$=current, initial, and maximum second invariants of the deviatoric stress tensor; I_1 and I_{10}=first invariants of the stress tensor at the current and initial states; f and g=material parameters that vary as a function of D_R; and n_g=material parameters representing effect of confining stress. There are several ways to obtain values of G_0 at small strain including empirical equations, laboratory tests and in situ tests. In this study, the following empirical equation, based on the work of Hardin and Black (1966), was used to estimate G_0 for various soil states

$$G_0 = C_g \frac{(e_g - e_0)}{1+e_0} p_A^{(1-n_g)} (\sigma'_m)^{n_g} \tag{9}$$

where C_g, n_g, and e_g=intrinsic material variables; e_0=initial void ratio; p_A=reference pressure=100 kPa; and σ'_m=initial mean effective stress in the same unit as p_A.

In order to describe failure and post-failure soil responses, the Drucker–Prager failure criterion was adopted. It has been well

known that the peak friction angle ϕ_p, defined in terms of the critical state friction angle ϕ_c and the peak dilatancy angle ψ_p, is a stress- and density-dependent variable (Bolton 1986). While ϕ_c is an intrinsic soil variable, independent of stress state, history, and density, ψ_p varies with both relative density and confinement. As a result, the envelope of the peak failure surface is nonlinear.

In this study, the following relationship proposed by Bolton (1986) was used to estimate the peak friction angle ϕ_p in sand:

$$\phi_p = \phi_c + 0.8\psi_p \tag{10}$$

where ϕ_p=peak friction angle; ϕ_c=critical state friction angle; and ψ_p=peak dilatancy angle=$6.25 \cdot I_R$ and $3.75 \cdot I_R$ for plane-strain and triaxial conditions, respectively. The dilatancy index I_R is given by

$$I_R = I_D\left[Q - \ln\left(\frac{100p'_p}{p_A}\right)\right] - R \tag{11}$$

where I_D=relative density (as a number between 0 and 1); p_A =reference pressure=100 kPa; p'_P=mean effective stress at peak strength in the same units as p_A; and Q and R=intrinsic soil variables. Eqs. (10) and (11) were used to define the nonlinear Drucker–Prager failure surface in the numerical simulation of footing load responses.

Numerical Modeling of Footing Load Tests

The finite element (FE) method was used to model axially loaded circular footings on sands. The commercial FE program *ABAQUS* was used to model the footing load tests, with a subroutine specifically written for the nonlinear stiffness and strength model described previously. Eight-noded axisymmetric elements were used in the finite element meshes to model both soils and the footings. For realistic numerical simulation of footing load response, the variation of ϕ_p of the foundation soil with confining stress must be considered. Even for a homogeneous deposit of constant D_R, the peak friction angle ϕ_p would vary with depth due to different confining stresses. At the same depth, ϕ_p would also vary with footing size as a result of the different stress states generated by the footing. The friction angle ϕ_p in our finite element analyses is therefore a variable, reflecting depth, stress state and footing size, rather than a constant value.

The degree of roughness between the footing base and soil is another factor to be addressed in the analysis. It is reasonable to expect that values of N_γ increase as the footing roughness increases. While many authors proposed values of N_γ for rough and smooth conditions separately, the actual footing condition would be neither perfectly rough nor perfectly smooth. Accordingly, in order to realistically model footing roughness, interface elements were used between the footing base and soil with a Coulomb friction coefficient of 0.7, corresponding to an interface friction angle equal to about 35°. This interface allows sliding between the footing and the soil whenever the interface shear strength is exceeded.

Measured and Predicted Footing Loading Responses

In order to validate the finite element analysis, field test results on axially loaded footings in sands were selected from the literature for comparison with finite element predictions. Footing load tests were performed at Texas A&M Univ. for the Settlement '94 ASCE Special Conference (Briaud and Jeanjean 1994). Square footings with four different sizes were tested: 1×1, 1.5×1.5, 2.5×2.5, and 3×3 m footings. The test site consists predominantly of sands down to a depth of 11 m. Beneath this sand layer, there is a very stiff clay deposit extending down to a depth of approximately 33 m. The water table was found at a depth equal to around 4.9 m.

As the test footings were square, both footings and soils were modeled with 20-noded three-dimensional (3D) solid elements instead of axisymmetric elements. Interface elements were used between footings and the surrounding soil. As the test footings were embedded 0.76 m into the soil, the same embedment was modeled in the finite element analyses for all the footings. This embedment corresponds to a soil overburden pressure equal to approximately 11.6 kPa. The initial stress states for the analyses were set as geostatic, based on unit weights estimated from the information obtained from the site characterization. All the soil properties used in the finite element analysis were those obtained from the site characterization and laboratory tests performed before the conference and provided in Briaud and Jeanjean (1994). Fig. 2 shows the measured and predicted footing load responses, where q_b represents the footing unit load. For comparison, load–settlement results using Schmertmann's method (Schmertmann et al. 1978) are also plotted. As can be seen in the figure, predictions using the nonlinear FE analyses show reasonably good agreement with measured results.

Footing Bearing Capacity for Various Soil States

Development of Footing Load–Settlement Curves

In order to obtain footing bearing capacities for a variety of soil states and footing sizes, a series of FE analyses were performed. Footings of different diameters (B=1, 2, and 3 m) with stiffness much greater than that of the soil were modeled as resting on the soil surface with no surcharge. The soil was assumed to be Ottawa sand, whose properties have been widely studied. Four different relative densities (D_R=30, 50, 70, and 90%) and three lateral earth pressure ratios (K_0=0.45, 0.70, and 1.00) were used in the analyses. The construction of the finite element models was done in a manner similar to that described in the previous section. The lateral and bottom boundaries of the finite element meshes were located at 12 m horizontally and 15 m vertically from the center of the footing base, respectively. Based on analyses with meshes of various sizes, it was found that the mesh size used in this study, extending laterally to more than four times the footing diameter and vertically to more than five times the footing diameter, is large enough to eliminate boundary effects. Interface elements were also used between the footing base and the soil, with a Coulomb friction coefficient of 0.7, corresponding to a friction angle equal to about 35°. Fig. 3 shows a typical finite element mesh used in this study.

Fig. 4 shows load-settlement curves from the finite element footing load analyses for different footing sizes (B=1, 2, and 3 m) and relative densities (D_R=30, 50, 70, and 90%) under K_0 =0.45. All the load–settlement curves were developed up to a settlement level equal to 20% of the footing diameter (i.e., s/B =0.2), corresponding to 20, 40, and 60 cm for the 1, 2, and 3 m footings, respectively. The footing unit load q_b at s/B=0.2 is taken here, for simplicity, as the limit unit bearing capacity q_{bL} of the footing. Note that this is not strictly the limit unit bearing capacity q_{bL} of the footing, particularly in dense sands, for which a considerable increase in bearing capacity is still possible after 20% settlement; however, this larger bearing capacity is ulti-

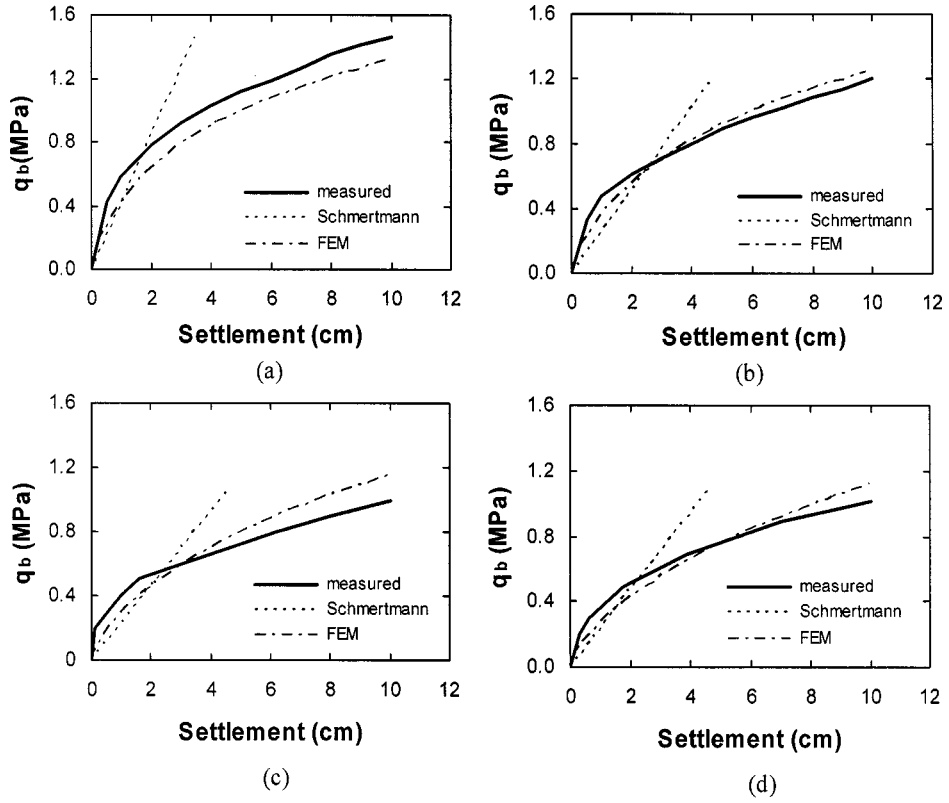

Fig. 2. Measured and predicted footing load–settlement curves for: (a) 1 m footing, (b) 1.5 m footing, (c) 2.5 m footing, and (d) 3 m footing

mately irrelevant for practical purposes, given the large settlements associated with it. Footing load responses for soils of $K_0 = 0.70$ and 1.00 were also developed using the same footing diameters and relative densities as used for $K_0 = 0.45$. Although not shown here, the shapes of the load–settlement curves for $K_0 = 0.70$ and 1.00 are similar to those for $K_0 = 0.45$.

Fig. 5 shows values of limit unit bearing capacity q_{bL} obtained from the finite element analysis for different footing diameters and soil states. It is observed that the effect of D_R on the limit unit bearing capacity q_{bL} is significant, while that of K_0 is relatively small, which is as expected based on considerations made earlier in the paper. This result provides support for neglecting K_0 effects, as most bearing capacity solutions do.

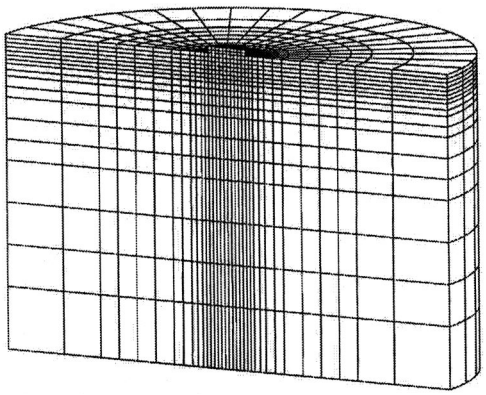

Fig. 3. Finite element mesh for axially loaded circular footing

Bearing Capacities from Finite Element Method and Bearing Capacity Factors

The limit unit bearing capacity values obtained from the finite element analysis in this study were compared with those calculated using the bearing capacity factor N_γ. Selected N_γ values for the comparison include those of Brinch Hansen (1970), Vesic (1973), Bolton and Lau (1993), and Michalowski (1997). The N_γ values of Michalowski (1997) are based on upper bound limit analysis, while those by Brinch Hansen (1970), Vesic (1973), and Bolton and Lau (1993) are based on limit equilibrium solutions.

Table 1 shows values of N_γ calculated following Brinch Hansen (1970), Vesic (1973), Bolton and Lau (1993), and Michalowski (1997) as a function of the friction angle ϕ. The N_γ values by Bolton and Lau (1993) differ significantly depending on whether smooth or rough conditions are assumed. As discussed before, the actual footing base condition would be neither completely smooth nor rough. Hence, the average of the N_γ values calculated by Bolton and Lau (1993) for smooth and rough conditions is also given in the table.

Fig. 6 shows limit bearing capacities q_{bL} of footings obtained from the finite element analysis and the various N_γ values for $K_0 = 0.45$. The friction angles ϕ for the determination of N_γ values in Fig. 6 were obtained from Eqs. (10) and (11) for the soil states considered. This requires the values of relative density D_R, which are known, and peak mean effective stress p'_p. Several different expressions have been suggested for the estimation of p'_p for use in connection with the bearing capacity problem (Meyerhof 1950; De Beer 1965; Perkins and Madson 2000). In this study, the following relationship by Perkins and Madson (2000) is used:

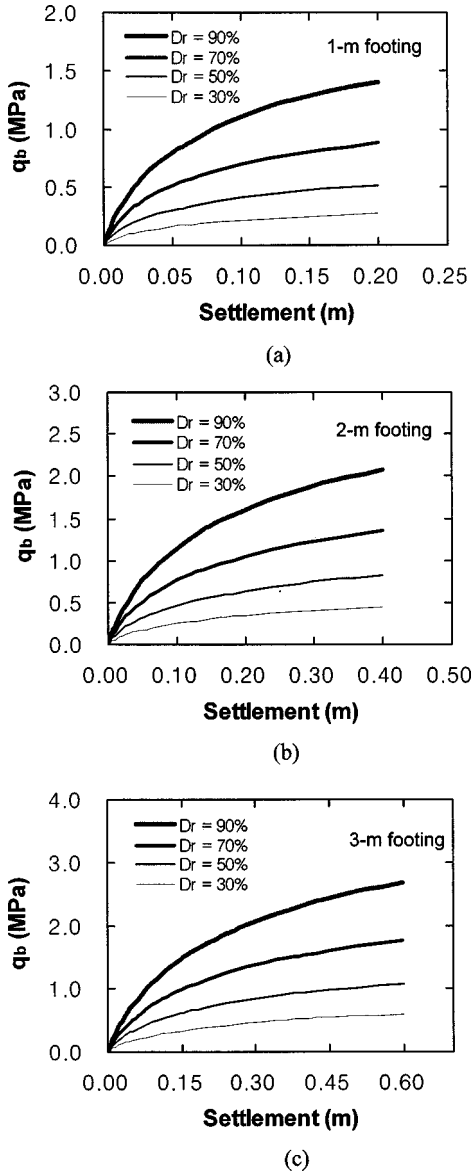

Fig. 4. Load–settlement curves with $K_0=0.45$ for: (a) 1 m footing, (b) 2 m footing, and (c) 3 m footing

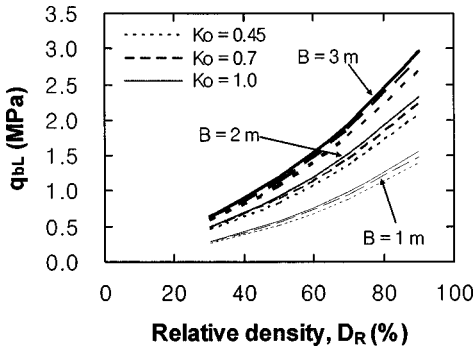

Fig. 5. Limit unit bearing capacity for different values of D_R, K_0, and footing diameter B

$$\frac{p'_p}{q_{bL}} = \frac{1}{6}\left(0.52 - 0.04\frac{L}{B}\right) \tag{12}$$

where p'_p=peak mean effective stress; q_{bL}=limit unit bearing capacity; and L and B=length and width of footing, respectively. The use of Eq. (12) is primarily due to simplicity while producing general agreement with previously published work and flexibility for 3D stress conditions, as explained by Perkins and Madson (2000). Values of q_{bL} in Eq. (12) for different methods were obtained iteratively with N_γ values corresponding to each method shown in Fig. 6. As shown in the figure, depending on the values of N_γ, large variations in q_{bL} are observed. It is seen that the values of q_{bL} calculated using N_γ by Bolton and Lau (1993) for the rough case are significantly greater than those from the finite element analysis. Use of N_γ values from Brinch Hansen (1970), Vesic (1973), Michalowski (1997), and Bolton and Lau (1993) for the smooth case, on the other hand, produces smaller q_{bL} values than the finite element results. Use of N_γ values obtained by averaging the smooth and rough base values of N_γ from Bolton and Lau (1993) results in reasonable agreement with the finite element results. Similar results were observed for $K_0=0.70$ and 1.00.

Cone Penetration Test-Based Footing Bearing Capacity

Normalized Limit Unit Bearing Capacity q_{bL}/q_c

In order to obtain footing bearing capacity based on CPT cone resistance q_c, the load–settlement curves obtained from the finite element analysis were normalized in terms of the normalized footing unit load q_b/q_c and the relative settlement s/B. Values of q_c used to normalize the load–settlement curves were obtained from *CONPOINT*, which is a cone resistance analysis program (Salgado and Randolph 2001; Salgado 2003) that can be used to calculate the cone resistance q_c. The cone resistance q_c from *CONPOINT* is determined using cavity expansion theory. For uncemented granular soils, it is generally possible to write

$$q_c = \mathbf{q_c}(D_R, \sigma'_v, \sigma'_h) \tag{13}$$

where $\mathbf{q_c}$=function containing intrinsic variables; D_R=relative density of sand before penetration; and σ'_v and σ'_h=initial vertical and lateral effective stresses. The details of the theoretical development, evaluation, and validation of the function represented by Eq. (13) are available in Salgado et al. (1997), Salgado and Randolph (2001), and Salgado (2003). The values of the intrinsic and state variables of the soil used in the *CONPOINT* analysis were the same as used in the finite element analysis.

The critical slip surface for footings is observed to extend to a depth, measured from the footing base, approximately equal to the footing diameter B. Accordingly, cone resistance values used to normalize the load–settlement curves were average cone resistances $q_{c,\text{avg}}$ from the footing base to a depth B below the footing base. The load–settlement curves for $K_0=0.70$ and 1.00 were normalized in the same way.

Fig. 7 shows normalized footing unit load q_b/q_c versus relative settlement s/B for $K_0=0.45$ and different values of D_R and B. Normalized load–settlement curves for $K_0=0.70$ and 1.00 were also developed. From the normalized load–settlement curves, values of the normalized limit unit bearing capacity q_{bL}/q_c were determined at $s/B=0.2$.

Table 1. Values of N_γ Proposed by Different Authors

ϕ'	Brinch Hansen (1970)	Vesic (1973)	Bolton and Lau (1993)			Michalowski (1997)
			Smooth	Rough	Average	
20	2.95	5.39	1.30	6.04	3.67	4.52
25	6.76	10.8	3.00	13.5	8.25	9.77
30	15.1	22.4	7.10	31.9	19.5	21.3
32	20.8	30.2	10.3	46.1	28.2	29.4
34	28.8	41.0	15.2	67.6	41.4	40.9
36	40.1	56.3	22.0	101	61.5	57.5
38	56.2	78.0	33.0	153	93.0	81.9
40	79.5	109	51.0	238	144	118
42	113	155	78.0	379	228	173
44	165	224	125	619	372	259
46	244	330	210	1,052	631	398
48	368	496	353	1,847	1,100	626
50	568	762	621	3,403	2,012	1,017

Effects of K_0 and D_R on Normalized Limit Unit Bearing Capacity q_{bL}/q_c

As discussed earlier, the influence of D_R on the limit unit bearing capacity q_{bL} is significant while that of K_0 is small to negligible. For the normalized limit unit bearing capacity q_{bL}/q_c, however, effects of both D_R and K_0 are found to be significant. Fig. 8 shows values of normalized limit unit bearing capacity q_{bL}/q_c for a 1 m footing as a function of D_R and K_0. From the figure, it is observed that values of q_{bL}/q_c decrease as D_R increases and that the rate of decrease depends on the value of K_0. At D_R=30%, values of q_{bL}/q_c are equal to 0.36 and 0.25 for K_0=0.45 and 1.00, while those at D_R=90% are 0.22 and 0.20, respectively. This indicates that the effect of K_0 on q_{bL}/q_c becomes smaller as D_R increases. The dependence of q_{bL}/q_c on K_0 is mainly due to the dependence of the cone resistance q_c on the horizontal effective stress σ'_h (and thus, on K_0). It is known that the horizontal effective stress σ'_h rather than the vertical effective stress σ'_v is a key variable along with the D_R in the determination of q_c (Salgado et al. 1997). As a result, the normalized limit unit bearing capacity q_{bL}/q_c shows a strong dependence on K_0, while the limit unit bearing capacity q_{bL} is insensitive to K_0.

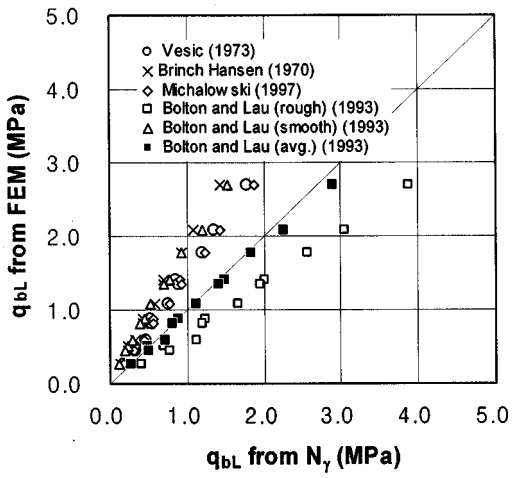

Fig. 6. Comparison of q_{bL} from finite element analyses and bearing capacity equation

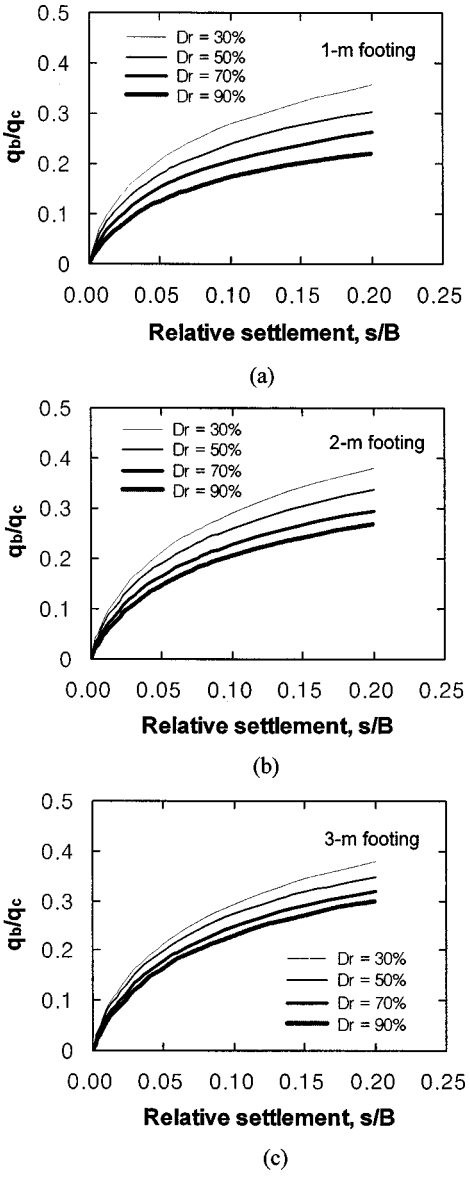

Fig. 7. Normalized load–settlement curves in terms of q_{bL}/q_c and s/B for: (a) 1 m footing, (b) 2 m footing, and (c) 3 m footing

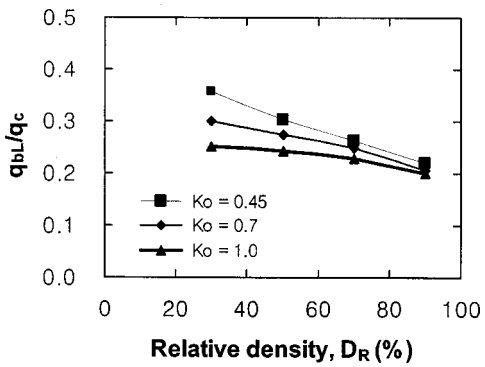

Fig. 8. Normalized limit unit bearing capacity q_{bL}/q_c with D_R and K_0

The issue of scale effects in the bearing capacity of footings, particularly with respect to the factor N_γ, must also be addressed. Several authors investigated scale effects in bearing capacity (Perkins and Madson 2000; Zhu et al. 2001). It is observed that the limit unit bearing capacity q_{bL} does not increase linearly with increasing footing size B, as the bearing capacity equation would appear to suggest. This scale effect is primarily due to the magnitude of the mobilized soil friction angle. As the footing size increases, producing larger confining stresses in the soil, the mobilized friction angle decreases, resulting in nonlinear increases of q_{bL} with B. Similar trends are observed in the normalized limit unit bearing capacity. Fig. 9 shows values of q_{bL}/q_c as a function of the footing diameter B. As shown in the figure, the normalized limit unit bearing capacity q_{bL}/q_c increases nonlinearly with increasing footing diameter B. However, it should be noticed that the scale effect for q_{bL}/q_c is not as significant as for q_{bL}, since the normalization based on $q_{c,\text{avg}}$ within an influence depth equal to B already reflects, in part, the effects of the size of the footing.

Allowable Footing Unit Load at Common Design Settlements

In design, settlement considerations often control. The tolerable settlement s_{tol} for shallow foundations is commonly assumed as 25 mm (or 1 in) with some variation depending on the importance of the structure (Terzaghi and Peck 1967; Becker 1996). Fig. 10 shows values of allowable footing unit load $q_{b,\text{all}}$ at $s_{\text{tol}}=25$ mm as

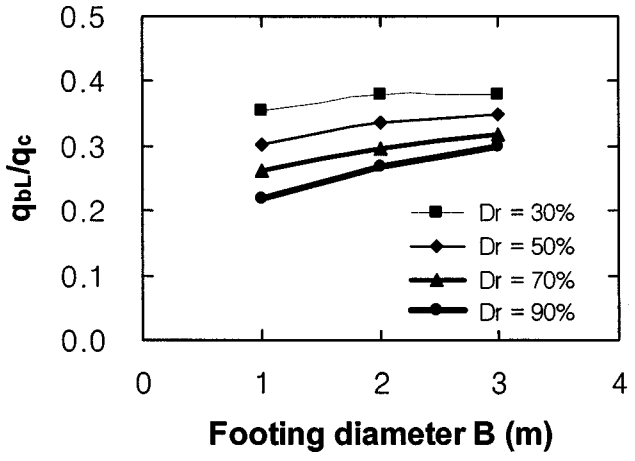

Fig. 9. Normalized limit unit bearing capacity q_{bL}/q_c versus footing diameter B

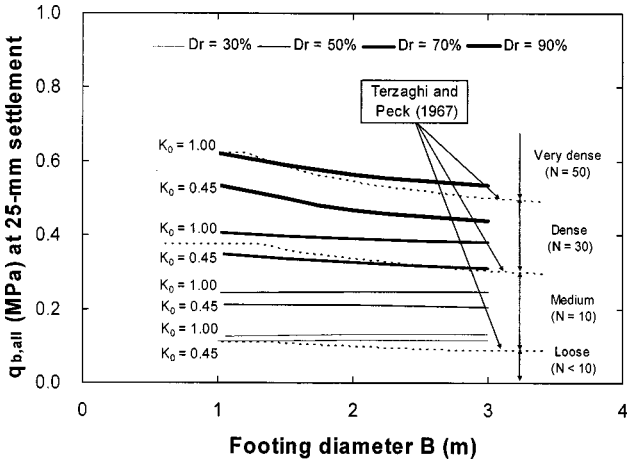

Fig. 10. Allowable footing unit load $q_{b,\text{all}}$ at 25 mm settlement versus footing diameter from finite element analyses and field test results

a function of soil density [as reflected by D_R and standard penetration test (SPT) blow counts N] and footing size. The solid lines are from our finite element analysis; the dashed lines are from field test results by Terzaghi and Peck (1967).

As can be seen in the figure, $q_{b,\text{all}}$ becomes more sensitive to footing size as D_R increases. At $D_R=90\%$, values of $q_{b,\text{all}}$ at $s_{\text{tol}}=25$ mm are 0.54, 0.47, and 0.44 MPa for the 1, 2, and 3 m footings under $K_0=0.45$, respectively, while at $D_R=30\%$ $q_{b,\text{all}}$ is insensitive to footing size. It is also shown that the effect of K_0 on the value of $q_{b,\text{all}}$ is greater at higher D_R values. From the results of Fig. 10, it is seen that results obtained in this study match well the results from the field tests of Terzaghi and Peck (1967), both of which show increasing dependence of $q_{b,\text{all}}$ on footing size as the D_R increases.

Normalized allowable unit load $q_{b,\text{all}}/q_c$ at 25 mm settlement was also obtained. Fig. 11 shows values of $q_{b,\text{all}}/q_c$ at the 25 mm settlement as a function of B, D_R, and K_0. As shown in the figure, values of $q_{b,\text{all}}/q_c$ decrease with increasing footing diameter. The size effect observed in Fig. 11 is consistent with that for the allowable footing unit load $q_{b,\text{all}}$ shown in Fig. 10. The influence of K_0 on values of $q_{b,\text{all}}/q_c$ was, however, different, depending on the values of D_R. At $D_R=90\%$, values of $q_{b,\text{all}}/q_c$, shown as thick lines in Figs. 11(a–c), are in nearly the same range of 0.05–0.08 for all the values of K_0 considered. At $D_R=30\%$, on the other hand, values of $q_{b,\text{all}}/q_c$ shown as thin lines in Figs. 11(a–c) decrease as K_0 increases. Note that if $s_{\text{tol}}=25$ mm, serviceability always controls for $B=1-3$ m, as $q_{b,\text{all}}/q_c$ is always less than q_{bL}/q_c.

Design Application

Estimation of the normalized limit unit bearing capacity q_{bL}/q_c for circular footings in sands can be made directly by applying the results of Figs. 8 and 9 for a given soil state and footing size. The CPT-based bearing capacity obtained in this study can be expressed as follows:

$$q_{bL}=\beta\cdot q_{c,\text{avg}} \tag{14}$$

where q_{bL}=limit unit bearing capacity; β=correlation factor; and $q_{c,\text{avg}}$=average cone resistance from the footing base to a depth measured from the footing base equal to the footing diameter B. Based on the results of Figs. 8 and 9, values of β are determined

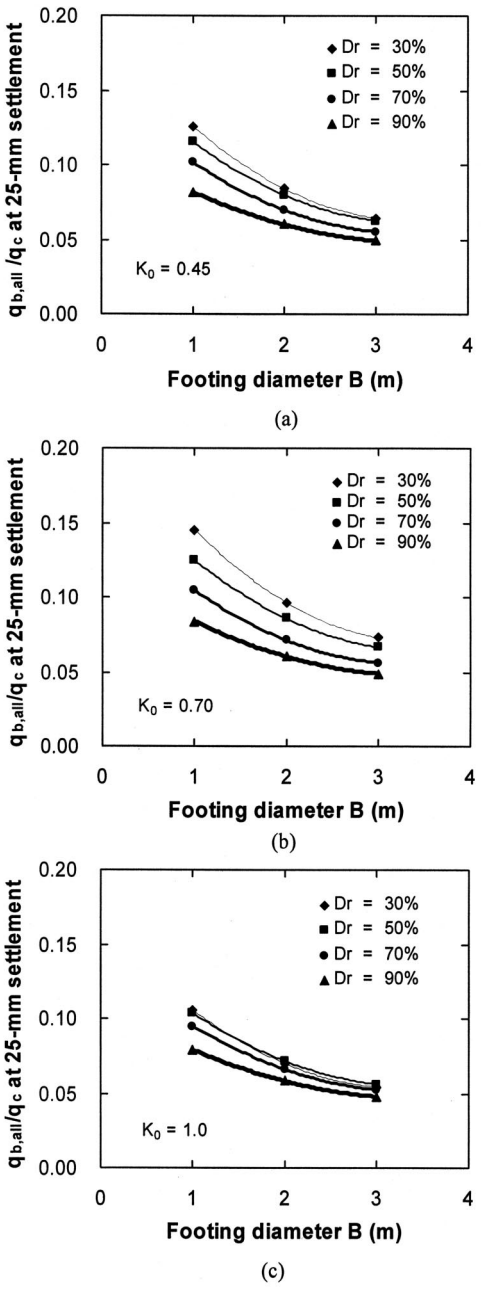

Fig. 11. Normalized allowable unit load $q_{b,all}/q_c$ at 25 mm settlement versus footing diameter B for: (a) $K_0=0.45$, (b) $K_0=0.70$, and (c) $K_0=1.00$

and summarized in Table 2. As shown in Fig. 9, the effect of footing size appears to be more significant as the D_R increases. Although some increase of β with increasing B is observed for looser soils (i.e., $D_R \leqslant 50\%$), this increase may be ignored for practical purposes. Consequently, the values of β in Table 2 reflect size effects only for denser sands (i.e., $D_R \geqslant 70\%$).

Tand et al. (1995) and Eslaamizaad and Robertson (1996) also proposed equations similar to Eq. (14) (Lunne et al. 1997). Most existing equations, however, do not include the effects of soil state as expressed by the relative density D_R and the lateral earth pressure ratio K_0 on the values of β. For instance, values of β according to Tand et al. (1995) vary from 0.14 to 0.2 in terms of footing shape and depth. Briaud and Jeanjean (1994) proposed a value of β equal to 0.25 based on the Texas A&M footing load test results previously described. It is noticeable that the value of β equal to 0.25 proposed by Briaud and Jeanjean (1994) corresponds to a value of β from Table 2 corresponding to a lightly to moderately overconsolidated ($K_0 \approx 0.45-0.7$), medium dense ($D_R \approx 70\%$) sand, which correspond to a soil state that is indeed similar to the actual soil state at the Texas A&M site, where their load tests were performed.

The results given in Table 2 are for circular footings on sands without a surcharge. Application of the results to square footings is possible with minimal error so long as an equivalent area is considered. For footing shapes other than circular or square, introduction of shape factors would be required.

Examples

In order to illustrate the use of the proposed method, a second site was selected from the literature (Lee et al. 2003) and used for the estimation of footing bearing capacity. The soil at the site is a predominantly gravelly sand down to a depth of around 13–14 m. Results from the site investigation indicate that the first 3 m of the gravelly sand deposit are in a loose state ($D_R \approx 30-40\%$, $\gamma \approx 16.5$ kN/m^3, and $\phi_c \approx 33°$), while the rest of the deposit down to a depth of 13–14 m is in dense to very dense states ($D_R \approx 80\%$, $\gamma \approx 18.0$ kN/m^3, and $\phi_c \approx 33°$). Soils near the surface are likely overconsolidated due to removal of a pavement and fill materials that existed there previously before the cone penetration tests and the rest of the ground characterization were conducted. Three circular footings, with diameters equal to 1, 2, and 3 m, are considered in this example.

The method proposed in this study can be used for estimating the bearing capacity of these footings by following these steps:

1. estimation of representative values of relative density D_R and lateral earth pressure ratio K_0 within the influence depth below the footing base (equal to the footing diameter B);

Table 2. Values of β for Cone Penetration Test-Based Bearing Capacity Assessment

D_R		β		
		$K_0=0.45$	$K_0=0.70$	$K_0=1.00$
30%		0.36	0.29	0.25
50%		0.30	0.27	0.24
70%	$B=B_r$[a]	0.26	0.25	0.23
	$B>B_r$[a]	0.26 $(0.90+0.10B/B_r)$	0.25 $(0.92+0.08B/B_r)$	0.23 $(0.94+0.07B/B_r)$
90%	$B=B_r$[a]	0.22	0.21	0.19
	$B>B_r$[a]	0.22 $(0.85+0.15B/B_r)$	0.21 $(0.85+0.15B/B_r)$	0.19 $(0.85+0.15B/B_r)$

[a]Reference footing diameter = 1 m ≈ 3.28 ft.

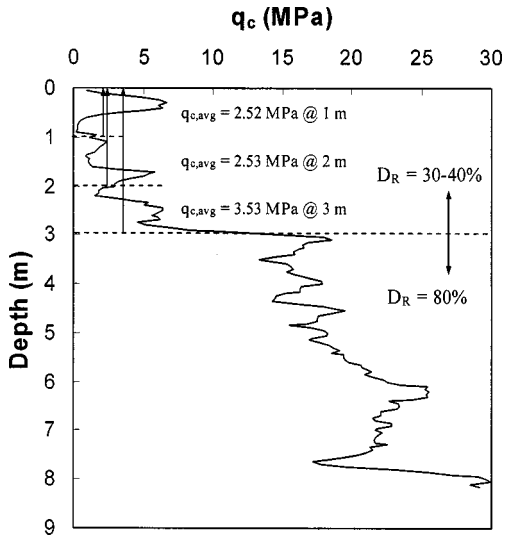

Fig. 12. Cone penetration test results used in q_{bL} calculation example

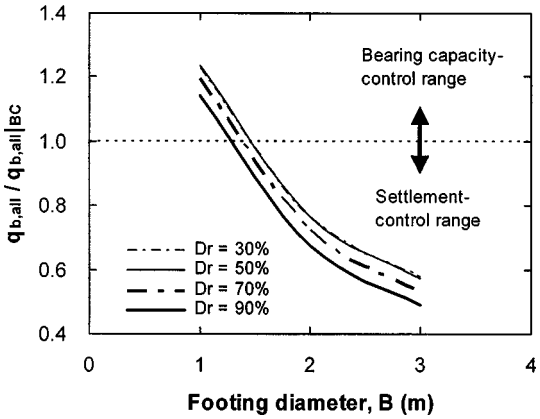

Fig. 13. Values of $q_{b,all}/\ q_{b,all|BC}$ with footing size and relative density

2. determination of β from Table 2 for the given values of D_R and K_0;
3. estimation of average cone resistance $q_{c,avg}$ within the influence depth (equal to B); and
4. determination of limit unit bearing capacity q_{bL} using Eq. (14).

Fig. 12 shows the q_c profile obtained from cone penetration testing performed at the site. From Table 2, the value of β was estimated as 0.31 (corresponding to D_R equal to 30–40% and K_0 value equal to around 0.6–0.7, with assumed overconsolidation ratio equal to around 2–3 to account for the surface overconsolidation condition). No size correction is necessary, as the relative density is lower than 50%. As shown in Fig. 12, values of $q_{c,avg}$ within the influence depths are 2.52, 2.53, and 3.53 MPa for 1, 2, and 3 m footings, respectively. From the values of β and $q_{c,avg}$, the values of limit unit bearing capacity q_{bL} were estimated as 0.78, 0.79, and 1.09 MPa for the 1, 2, and 3 m footings, respectively.

For comparison purposes, q_{bL} was also estimated using the bearing capacity factor N_γ. The values of N_γ according to the equation put forth by Vesic (1973) were 79.9, 71.3, and 66.7 for the 1, 2, and 3 m footings, respectively. These values were obtained based on peak friction angles ϕ_p equal to 38.2, 37.5, and 37.1° estimated from Eqs. (10)–(12) with $D_R \approx 30-40\%$, $\gamma \approx 16.5$ kN/m^3, and $\phi_c \approx 33°$. Calculated values of q_{bL} are then 0.40, 0.71, and 0.99 MPa for the 1, 2, and 3 m footings, respectively. Compared with the values obtained using the proposed method, these are conservative, particularly for the 1 m footing. If a factor of safety (FS) equal to 3.0 is introduced, values of the allowable unit bearing capacity $q_{b,all|BC}$ are 0.13, 0.24, and 0.33 MPa for the 1, 2, and 3 m footings, respectively.

From Fig. 10, it can seen that the value of $q_{b,all|BC} = 0.13$ MPa for the 1 m footing is close to the value of the allowable footing unit load for a 25 mm settlement, $q_{b,all} \approx 0.12$ MPa, corresponding to $B=1$ m and $D_R=30\%$. For the larger footings (i.e., $B=2$ and 3 m), on the other hand, the values of $q_{b,all|BC}$ equal to 0.24 and 0.33 MPa are greater than values of $q_{b,all}$ shown in Fig. 10 by a large margin. This indicates that, as the footing size and relative density decrease, the limit bearing capacity limit state controls design, while the settlement-based allowable unit load $q_{b,all}$ controls for larger footings in denser soils. This result is also shown in Fig. 13, in which the ratio of $q_{b,all}$ to $q_{b,all|BC}$ (calculated by dividing q_{bL} by FS=3.0) is plotted as a function of footing size B and relative density D_R. Values of q_{bL} and $q_{b,all}$ used in Fig. 13 are those from Figs. 5 and 10 for $K_0=0.45$. In the figure, when $q_{b,all}/q_{b,all|BC} > 1.0$ bearing capacity controls and when $q_{b,all}/q_{b,all|BC} < 1.0$ settlement controls. This chart is not universally applicable; it would change as different values of s_{tol} and FS are used, but it shows that settlement would tend to control design quite often.

Summary and Conclusions

In the present study, estimation of the bearing capacity of circular footings on sands based on CPT cone resistance q_c was investigated. A conventional check of the bearing capacity limit state using the bearing capacity equation requires calculation of N_γ and thus an estimate of ϕ. Significant uncertainties exist in the values of N_γ and the soil friction angle ϕ. The CPT-based bearing capacity analysis of this study does not require estimates of ϕ or N_γ; bearing capacity is determined directly from the CPT cone resistance.

In order to simulate the loading response of axially loaded circular footings in sands, the finite element method was used with a subroutine written for the non-linear elastic–plastic stress–strain model of Lee and Salgado (2000). Various soil states, including four different relative densities ($D_R=30$, 50, 70, and 90%) and three different lateral stress ratios ($K_0=0.45$, 0.70, and 1.00), were considered. The footings were modeled as elastic with three different diameters ($B=1$, 2, and 3 m). As the footing base is neither perfectly smooth nor perfectly rough, interface elements between the footing and soil were used. Based on the finite element results, load–settlement curves were developed and used to determine the limit unit bearing capacity q_{bL} for various soil and footing conditions.

In order to obtain the normalized limit unit bearing capacity q_{bL}/q_c, the load–settlement curves obtained from the finite element analysis were normalized with respect to cone resistance q_c. The cone resistance q_c used for the normalization was an average value for the influence zone extending from the footing base to a depth equal to the footing diameter B below the footing base. Values of q_{bL}/q_c were found to be in a range of 0.20–0.36, depending on the values of D_R, K_0, and B. It was found that both the relative density D_R and the lateral earth pressure ratio K_0 are

important factors affecting the value of the normalized limit unit bearing capacity q_{bL}/q_c. The normalized limit unit bearing capacity q_{bL}/q_c decreases as D_R increases, with the rate of decrease depending on the K_0 values. The effect of K_0 was greater for lower D_R values.

There is a size effect on the values of q_{bL}/q_c. The size effect increases as the footing diameter B increases. For D_R lower than about 50%, the size effect on q_{bL}/q_c may be ignored for practical purposes. Design values of the normalized limit unit bearing capacity were presented in equation, chart, and table formats.

The normalized allowable unit load $q_{b,\mathrm{all}}/q_c$ at 25 mm settlement was also studied. Results from the present analysis are in close agreement with field measurements. The normalized allowable unit loads at other settlement levels can also be determined based on the normalized load–settlement curves in terms of q_b/q_c versus s/B.

Notation

The following symbols are used in this paper:

B = footing width or diameter;
b_c, b_q, b_γ = base inclination factors;
C_g = small-strain shear modulus number;
c = cohesive intercept;
D_R = relative density (%);
d_c, d_q, d_γ = depth factors;
e_g = small-strain shear modulus void ratio number;
e_0 = initial void ratio;
f = material parameter in nonlinear stiffness model;
G = secant shear modulus;
G_0 = initial shear modulus;
g = material parameter in nonlinear stiffness model;
g_c, g_q, g_γ = ground inclination factors;
I_D = relative density as number between 0 and 1;
I_R = dilatancy index;
I_1 = first invariant of stress tensor at current state;
I_{10} = first invariant of stress tensor at initial state;
i_c, i_q, i_γ = load inclination factors;
J_2 = second invariant of deviatoric stress tensor at current state;
$J_{2\max}$ = second invariant of deviatoric stress tensor at failure;
J_{20} = second invariant of deviatoric stress tensor at initial state;
K_0 = coefficient of lateral earth pressure at rest;
L = footing length;
N_c, N_q, N_γ = bearing capacity factors;
n_g = small-strain shear modulus exponent;
p_A = atmospheric pressure;
p'_p = mean effective stress at peak strength;
Q = intrinsic soil variable in correlation for peak friction angle;
q = surcharge;
q_b = footing unit load;
$q_{b,\mathrm{all}}$ = allowable footing unit load;
$q_{b,\mathrm{all|BC}}$ = allowable unit bearing capacity of footing;
q_{bL} = limit unit bearing capacity of footing;
q_c = Cone penetration test cone resistance;
$q_{c,\mathrm{avg}}$ = average Cone penetration test cone resistance within influence depth;
R = intrinsic soil variable in correlation for peak friction angle;
s = footing settlement;
s_d, s_γ, s_q = shape factors;
s_{tol} = tolerable footing settlement;
s/B = relative settlement (settlement divided by footing size);
β = correlation factor between cone resistance and footing bearing capacity;
γ = soil unit weight;
σ'_h = horizontal effective stress;
σ'_m = mean effective stress;
σ'_v = vertical effective stress;
ϕ = friction angle;
ϕ_c = friction angle at critical state;
ϕ_p = peak friction angle; and
ψ_p = peak dilatancy angle.

References

Becker, D. (1996). "Eighteenth Canadian geotechnical colloquium: Limit states design for foundations Part 1. An overview of the foundation design process." *Can. Geotech. J.*, 33(6), 956–983.

Bolton, M. D. (1986). "The strength and dilatancy of sands." *Geotechnique*, 36(1), 65–78.

Bolton, M. D., and Lau, C. K. (1993). "Vertical bearing capacity factors for circular and strip footings on Mohr–Coulomb soil." *Can. Geotech. J.*, 30, 1024–1033.

Briaud, J. L., and Jeanjean, P. (1994). "Load settlement curve method for spread footings of sand." *Proc., Settlement '94, Vertical and Horizontal Deformations of Foundations and Embankments*, Vol. 2, ASCE, New York, 1774–1804.

Brinch Hansen, J. (1970). "A revised and extended formula for bearing capacity." *Bulletin No. 28*, Danish Geotechnical Institute, Copenhagen, Denmark.

Chen, W. F. (1975). *Limit analysis and soil plasticity*, Elsevier, Amsterdam, The Netherlands.

De Beer, E. E. (1965). "Bearing capacity and settlement of shallow foundations on sand." *Proc., of Bearing Capacity and Settlement of Foundation Symp.*, Duke Univ., Durham, N.C., 15–34.

Drucker, D., Prager, W., and Greenberg, H. (1952). "Extended limit design theorems for continuous media." *Q. Appl. Math.*, 9, 381–389.

Erickson, H. L., and Drescher, A. (2002). "Bearing capacity of circular footings." *J. Geotech. Geoenviron. Eng.*, 128(1), 38–43.

Eslaamizaad, S., and Robertson, P. K. (1996). "Cone penetration Test to evaluate bearing capacity of foundation in sands." *Proc. 49th Canadian Geotechnical Conf.*, St. John's, Newfoundland, Canada.

Frydman, S., and Burd, H. J. (1997). "Numerical studies of bearing-capacity factor N_γ." *J. Geotech. Geoenviron. Eng.*, 123(1), 20–29.

Griffiths, D. V. (1982). "Computation of bearing capacity factors using finite elements." *Geotechnique*, 32(3), 195–202.

Hardin, B. O., and Black, W. L. (1966). "Sand stiffness under various triaxial stresses." *J. Soil Mech. Found. Div.*, 92(2), 27–42.

Kumbhojkar, A. S. (1993). "Numerical evaluation of Terzaghi's N/G_g." *J. Geotech. Eng.*, 119(3), 598–607.

Lee, J. H., and Salgado, R. (2000). "Analysis of calibration chamber plate load tests." *Can. Geotech. J.*, 37(1), 14–25.

Lee, J. H., Salgado, R., and Paik, K. H. (2003). "Estimation of the load capacity of pipe piles in sand based on cone penetration test Results." *J. Geotech. Geoenviron. Eng.*, 129(5), 391–403.

Lunne, T., Robertson, P. K., and Powell, J. M. (1997). *Cone penetration testing in geotechnical practice*, E&FN Spon, London.

Meyerhof, G. G. (1950). "The bearing capacity of sand." PhD thesis, Univ. of London, London.

Michalowski, R. L. (1997), "An estimate of the influence of soil weight

on bearing capacity using limit analysis." *Soils Found.*, 37(4), 57–64.
Perkins, S., and Madson, C. (2000). "Bearing capacity of shallow foundations on sand: A relative density approach." *J. Geotech. Geoenviron. Eng.*, 126(6), 521–530.
Prandtl, L. (1921). "Über die Eindringungsfestigkeit (Härte) plastischer Baustoffe und die Festigkeit von Schneiden." *Z. Angew. Math. Mech.*, 1, 15–20.
Reissner, H. (1924). "Zum erddruckproblem." *Proc., 1st Int. Congress of Applied Mechanics*, Delft, The Netherlands, pp. 295–311.
Salgado, R. (2003). *CONPOINT manual*.
Salgado, R., Mitchell, J. K., and Jamiolkowski, M., (1997). "Cavity expansion and penetration resistance in sand." *J. Geotech. Geoenviron. Eng.*, 123(4), 344–354.
Salgado, R., and Randolph, M. F. (2001). "Analysis of cavity expansion in sands." *Int. J. Geomech.*, 1(2), 175–192.
Schmertmann, J. H., Brown, P. R., and Hartman, J. P. (1978). "Improved strain influence factor diagrams." *J. Geotech. Eng. Div., Am. Soc. Civ. Eng.*, 104(8), 1131–1135.
Sloan, S. W., and Yu, H. S. (1996). "Rigorous plasticity solutions for the bearing capacity factor N_γ." *Proc., 7th Australia–New Zealand Conf. on Geomechanics*, Adelaide, 544–550.
Soubra, A. (1999). "Upper-bound solution for bearing capacity of foundations." *J. Geotech. Geoenviron. Eng.*, 125(1), 59–68.
Tand, K. E., Funegard, E. G., and Warden, P. E. (1995). "Predicted/measured bearing capacity of shallow footings on sand." *Proc., Int. Symp. on Cone Penetration Testing, CPT'95*, Linkoping, Sweden, 589–594.
Terzaghi, K. (1943). *Theoretical soil mechanics*, Wiely, New York.
Terzaghi, K., and Peck, R. B. (1967). *Soil mechanics in engineering practice*, 2nd Ed., Wiley, New York.
Vesic, A. S. (1973). "Analysis of ultimate loads of shallow foundation." *J. Soil Mech. Found. Div.*, 99(1), 45–73.
Zhu, D. (2000). "The least upper-bound solutions for bearing capacity factor N_γ." *Soils Found.*, 40(1), 123–129.
Zhu, F., Clark, J. I., and Phillips, R. (2001). "Scale effect of strip and circular Footings resting on a dense sand." *J. Geotech. Geoenviron. Eng.*, 127(7), 613–621.